

CHAPTER 1

Introduction and Literature Review

CHAPTER 1

Introduction and Literature Review

1.1 Organic Electronics

Since the first report of organic field effect transistors (OFETs) in 1983, significant progress has been achieved in the field of organic semiconductors[3]. Compared with conventional inorganic semiconductors (like silicon, germanium, and III-V semiconductors), organic semiconductors can be processed at low temperature and ambient environment making them suitable candidates for flexible and low-cost electronics. This difference in processing temperature is because of the presence of strong covalent bonds in inorganic semiconductors while organic semiconductors have weak Vander Waal bonds[3], [4]. Fig. 1.1 shows some of the key milestones in the development of OFET devices followed by Figure 1.2 which highlights some common application areas of OFETs [1], [2]. Solution processing techniques like spin coating, and drop casting are more popular for organic semiconductors because of low cost and ease of processability[5]. Recently Floating film transfer method (FTM), another solution process technology for organic semiconductors, has gained attention because of the minimal material wastage of costly organic semiconductors, large-area processing suitability, and no requirement of sophisticated instruments. However, most reports exploiting the FTM for OFET fabrication have used ethylene glycol and glycerol as liquid substrate which is environmentally damaging, and waste disposal will harm the environment and human health. Furthermore, eco-friendly water can also be used as a liquid substrate in FTM. However,

reports utilizing water as a liquid substrate in FTM for OFET fabrication are rare. Considering the significant application of OFETs in portable sensors low voltage operation is another key requirement. High k dielectrics are commonly used to reduce the operating voltage. Several inorganic dielectrics like HfO_2 , TiO_2 , ZrO_2 , Ta_2O_5 , etc. have been commonly used with organic semiconductors. However, there are no reports on the exploitation of LiO_x as the gate dielectric for organic semiconductors [6], [7], [16]–[25], [8]–[15]. Another important aspect regarding inorganic dielectric processing is water-driven synthesis which is superior to synthesis using toxic organic solvents which are environmentally damaging. However, the reports of utilization of water driven inorganic dielectrics for OFETs are rare[26]–[31].

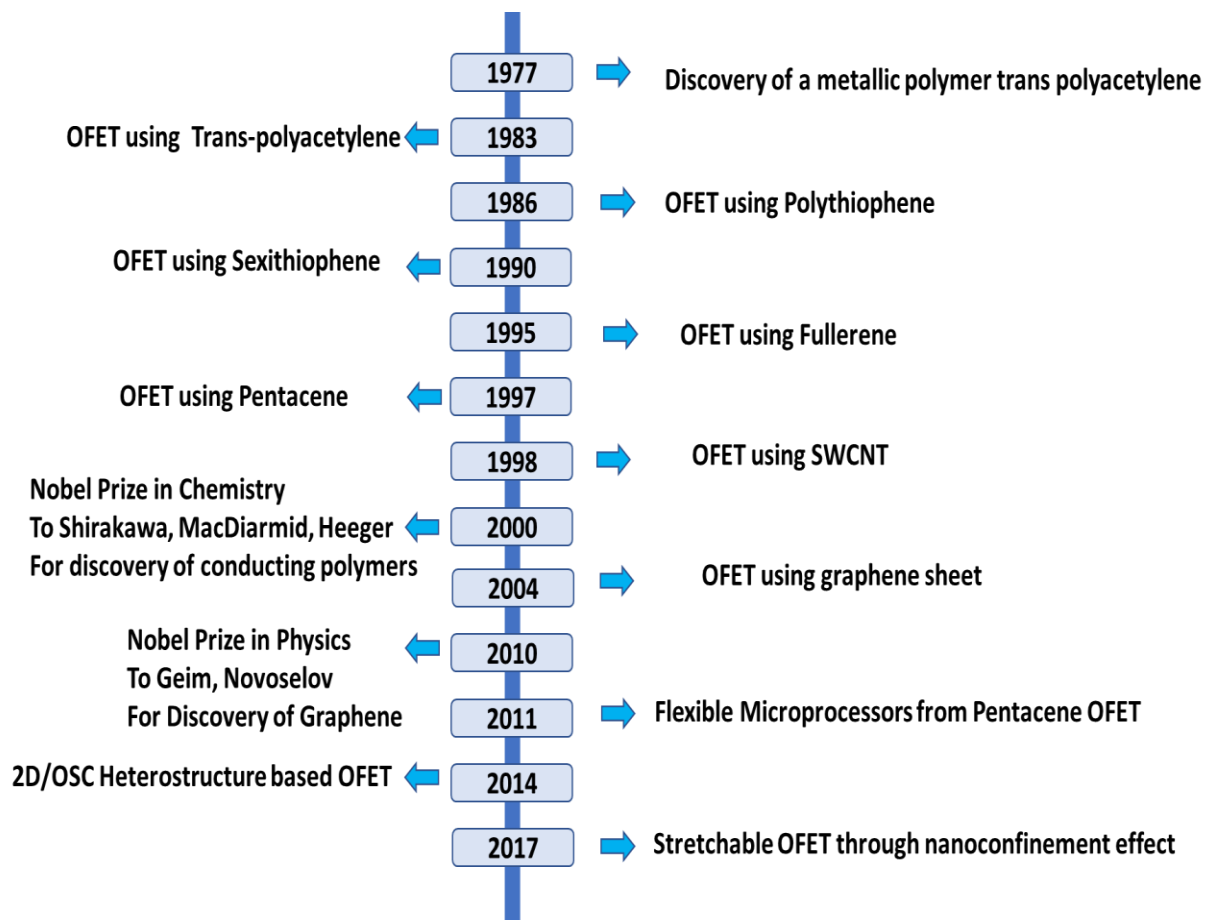


Figure 1.1 Historical Perspective of OFETs[1], [2].

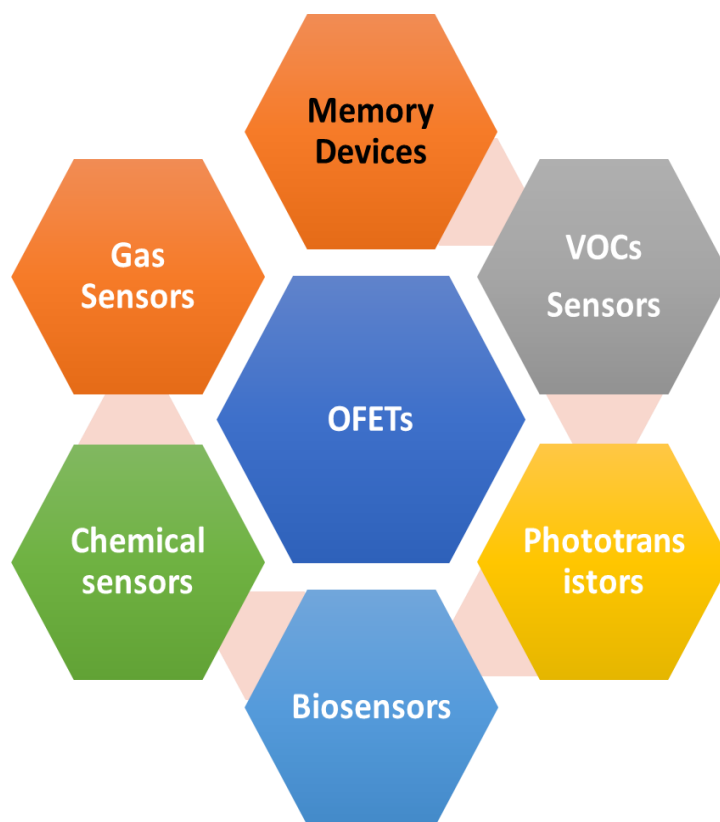


Figure 1.2 Applications of Organic Field Effect Transistors.

This thesis integrates the water-driven synthesis of inorganic dielectric with water transferred FTM film (W-FTM) of organic semiconductor (DPP-DTT) for low-voltage operable high-performance OFETs. Furthermore, the gas sensing (NO_2) and light sensing performance of W-FTM transferred DPP-DTT-based low voltage OFETs have been investigated. In this chapter, the state-of-the-art review, motivation, problem statement, objective, a brief introduction to

charge transport in OFETs, the basic structures of OFETs, performance parameters, and scope of the thesis have been covered.

1.2 State-of-the-Art Review

This section covers a brief literature review on the inorganic high k dielectrics for OFETs, water processed inorganic dielectrics, solution processed techniques for OFETs, NO_2 sensors based on OFETs, and near infrared organic phototransistors (NIR-OPTs).

1.2.1 Review of Some High k dielectric for OFETs

Conventional silicon dioxide based OFETs generally have very high operating voltage thereby making the SiO_2 based OFETs unsuitable for portable and low power applications. The two common strategies in the literature that have been extensively adopted to lower the operating voltage of OFETs are lowering the dielectric thickness or employing a high k dielectric. However, the strategy of lowering the thickness of dielectrics to increase the capacitance is generally not preferred as it increases the leakage current and reduces the breakdown voltage. The most commonly used high k dielectrics can be, broadly, classified based on their chemical nature namely, inorganic high k dielectrics and organic polymer based high k dielectrics. Recently many groups have used the Al_2O_3 , HfO_2 , ZrO_2 , TiO_2 , Ta_2O_5 , and Y_2O_3 as dielectric for OFETs to lower the operating voltage[10], [12], [24], [25], [13]–[17], [21]–[23]. However, the most common problem associated with inorganic dielectrics is surface trap charges, surface defects, and roughness thereby degrading the performance and electrical stability of OFETs. One interesting property of high k inorganic dielectrics is the inverse relation between the bandgap (E_g) and the k (dielectric constant) value, i.e., the larger the k value smaller the bandgap. On the other hand, a larger E_g value has its advantage as it helps in preventing charge

injection through electrodes and minimizing the generation of charges by photo or thermal excitations. Table 1.1 summarizes some state-of-the-art reviewed inorganic dielectrics-based OFETs.

TABLE 1.1 REVIEW OF HIGH K DIELECTRICS IN OFETS

Structure	μ_{\max} ($\text{cm}^2 \text{V}^{-1} \text{sec}^{-1}$)	$I_{\text{on}}/I_{\text{off}}$	SS (mV/ decade)	V_{TH} (V)	Deposition method (OSC/Dielectric)	V_{GS} (V)	Year Ref.
BZT/Pentacene	0.32	10^5	300	--	V/V (Sputtering)	-5	1999[14]
Ta ₂ O ₅ /P3HT	0.02	10^2	--	--	SC/V	-3	2002[12]
AlO _x /Penatcene	0.14	10^5	800		V/V		2003[22]
TiO _x /P3HT	0.015	10^2	--	-1	SC/SC	-5	2004[20]
TiO _x :PVP/Pentacene	0.24	10^3	--	-7	V/V	-40	2004[21]
Gd ₂ O ₃ /Pentacene	0.1	10^3	---	-3.5	V/V	-8	2004[13]
TiO _x :PS/Pentacene	0.22	10^2	---	-2.1	V/SC	-20	2005[15]
HfO _x /Pentacene	0.13	10^3	--	-0.75	V/SC	-2	2007[10]
AlO _x /ODPA/Pentacene	0.6	10^7	100	--	V/V	-3	2007[8]
HfO _x /PA/Pentacene	0.22	10^5	130	-0.53	V/SC	-1.5	2008 [17]
Zr-SAND/ Pentacene	0.38	10^5	--	-0.8	V/SC	-4	2011[25]

AlO _x /ODPA/TI PS	0.11	10 ⁶	130	-0.7	SC/V	-2	2011[9]
Structure	μ_{max} (cm² V⁻¹sec⁻¹)	I_{on}/I_o r	SS (mV/ deca de)	V_{TH} (V)	Deposition method (OSC/Dielectric)	V_{GS} (V)	Year Ref.
P(VDF-TrFE- CFE)/PBTTTC- 14	0.43	10 ⁶	97		SC/SC	-3	2012[7]
ZrO _x :CYLEP/P 3HT	0.08	10 ³	300	-0.8	SC/SC	-5	2013[16]
PI/AlO _x /C-10- BTBT	1.42	10 ⁵	420	-7	SC/SC	-30	2013[24]
ZrO _x /PBTTT C14	0.18	10 ⁵	115	-0.75	SC/SC	-3	2013 [32]
PVA-CR/TIPS- P	0.8	10 ⁴	100	-0.5	SC/SC	-3	2014[11]
AlO _x /PS/Pentac ene	0.51	10 ⁴	--	-2.1	V/SC	-6	2015[23]
PVA-AD/DF- P3HT	6.3	10 ³	1300	-1.9	FTM/SC	-5	2017[6]
HfO ₂ /PVP/TIPS	0.11	10 ⁵	810	0.08	V/SC/SC	-10	2017 [33]
HfO ₂ /PVA/TIPS	0.69	10 ³ - 10 ⁴	NA	-0.58	SC/V/SC	-10	2019 [34]

V: Vacuum Processing
 SC: Spin coating
 FTM: Floating Film Transfer Method

1.2.2 Review of water processed inorganic dielectrics:

This section covers a brief review of water processed inorganic dielectrics. Solution processing of inorganic dielectric is generally done using organic solvents like 2-methoxy ethanol (2-MEA), N, N-dimethylformamide (NMP), and dimethylformamide (DMF) as well as other organic additives. 2-ME, DMF, etc., and commonly used organic additives are toxic, environmentally damaging, and harmful to human health[29][27][28][30]. Some of the harmful effects of these solvents have been enlisted in Figure 1.3.

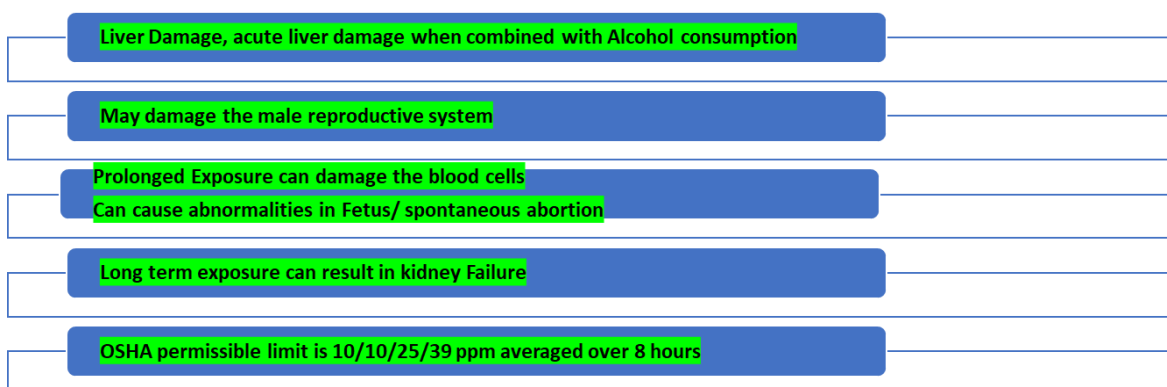


Figure 1.3 Health Hazards on Exposure to Dimethylformamide (DMF) /NMP/2-MEA/ Ethylene Glycol (EG) Vapors.

Water-based synthesis of inorganic dielectric has many advantages over the commonly used organic solvent-based synthesis [26], [28], [29], [35]: Some of the advantages, apart from eco-friendly nature, are enlisted here:

1. **No requirement of Vacuum or inert environment for storage of Precursor:** The precursor solutions using common organic solvents like 2-methoxyethanol (2-ME) or

DMF or NMP are sensitive to the moisture in the environment so it needs to be stored in the inert environment or vacuum. However, the water-based precursor solutions are insensitive to moisture fluctuations thereby eliminating the need for an inert storing environment/ vacuum for handling.

2. **Low thermal annealing:** Furthermore, comparatively lower thermal energy is required to break the weak coordinating bond that is formed between the metal cation and aqua ion than the covalent bond which is formed with organic solvents like 2-ME. Thus, the water-induced dielectric processing requires low annealing temperature in comparison to organic solvents.
3. **Smother Dielectric surface:** The use of toxic organic solvents (as additives or solvents) results in a higher annealing temperature and also results in the harmful emission of a comparatively higher number of volatile gases, which increases the roughness and film porosity of dielectric films, thereby increasing leakage current density and deteriorating OFET performance parameters.
4. **Low-cost Processing:** Furthermore, from a processing cost perspective, water is comparatively cost effective when compared with organic solvents and additives.

Liu et al [29] in 2015 demonstrated water induced AlO_x dielectric for indium oxide-based TFTs. They used an aluminum nitrate-based precursor and an annealing temperature of around 350°C . The water induced AlO_x layer showed a dielectric constant of ~ 7 and low leakage current density with a smoother surface. The processing temperature required for water induced AlO_x was much lower than that of the 2-ME based AlO_x . Liu et al in 2015[27] reported eco-friendly water induced high-k yttrium oxide (YO_x) dielectric for fully water induced indium oxide TFTs. No toxic additives were used in the YO_x precursor solution which when

annealed at 350°C showed extremely low leakage current ($\sim 2 \times 10^{-9}$ A/cm² at 5 MV/cm) and high capacitance density of ~ 448 nF/cm² (at 1 KHz). Liu et al in 2015[28] demonstrated water induced scandium oxide based indium oxide TFTs. Zhu et al in 2016 [30] reported water processed Zirconium oxide (ZrO_x) based Indium oxide TFTs. The annealing temperature of ZrO_x has been reduced from 500 °C in the case of 2-ME to 300 °C for water induction. The ZrO_x film annealed at 300 °C shows a capacitance value of 535 nF/cm² at a frequency of 1 KHz while an extremely low leakage current density of $\sim 10^{-9}$ A/cm² at 5 MV/cm was recorded. Zhu et al in 2018[31] demonstrated water induced ZrGdO_x dielectric for indium oxide TFT. The water induced ZrGdO_x annealed at 400 °C shows low leakage current density of $\sim 10^{-8}$ A/cm² 1 MV/cm while it showed areal capacitance of value of ~ 531 nF/cm² at 20 Hz. Zhu et al in 2019[36] demonstrated water driven synthesis of AlZrO_x dielectric for indium oxide TFT. AlZrO_x based dielectric annealed at 500 °C showed low leakage current density of $\sim 10^{-8}$ A/cm² at 1 MV/cm and areal capacitance of ~ 512.8 nF/cm² at 20 Hz with the surface roughness of ~ 0.29 nm. Thus, based on the discussion above and the brief literature survey covered, water-based processing of inorganic dielectric is superior to commonly used organic solvent-based processing in terms of annealing temperature, film roughness, environmental friendliness, and cost of processing.

1.2.3 Review of Deposition techniques for Organic semiconductors:

The processing techniques for organic semiconductors can be broadly classified as vacuum deposition and solution processing techniques. The solution processed technologies have low cost and ease of processing advantage over the costly vacuum deposition methods. Various solution process techniques like drop casting, spin coating, and inkjet printing have been widely used to process organic semiconductor film. These approaches, while simple to use,

have significant limitations such as limited region applicability and low film quality[5], [37]. The low quality of the processed film can be attributed to weak cohesive forces among molecules as a result of their random orientation during film processing. Another concern with these film processing procedures is the film's non-uniform thickness, which prevents strong adhesion of the film to the substrate and results in the disintegration of the film in numerous areas[38]. Recently Floating film transfer method is another solution processed technology that is gaining attention. This section will focus on the Floating film transfer method (FTM), a solution process technique suitable for large area electronics and cost effective processing[5], [37]–[39].

Floating Film Transfer Method:

The floating film transfer method (FTM) was first reported and developed by Kaneto and coworkers in 1979. FTM method generally consists of three steps described below [40], [41]:

1. A drop of the polymer solution (about 10 μL) is placed in the center of a petri dish containing an orthogonal liquid substrate (water in our case).
2. The polymer solution is then allowed to spread before the solvent evaporates.
3. Finally, the dried floating film is stamped onto any desired substrate.

A schematic describing these three steps have been depicted in Fig. 1.5. Ethylene glycol, glycerol, and, hydrophilic water is widely utilized as liquid substrates in the FTM process, because of their orthogonality to routinely used hydrophobic organic solvents (to dissolve the Organic semiconducting polymers). The floating film method

Detail of Floating Film Transfer Method

FTM which involves the process of spontaneous spreading (also known as Marangoni flow) generally occurs when a polymer solution possessing low surface energy (e.g., Hydrocarbon Solvents, Detergents) is dropped over the surface of the liquid substrate (Water or a mixture of Ethylene glycol and glycerol) having higher surface energy. This difference in surface energy of both the liquids leads to a local surface tension gradient further resulting in surficial flow towards areas with comparatively higher surface tension. Figure 1.4 represents the net spreading coefficient and all the surface tension forces acting on the polymer droplet. A parameter called spreading coefficient (S), which is based on the surface tensions at the three-phase contact line where a liquid droplet hits the liquid substrates, determines the rate of the spreading flow. Where Y_1 is the surface energy of water, Y_2 is the surface energy of the solution, Y_{12} is the interfacial surface energy, and S is the spreading coefficient. When the net spreading coefficient (S) is positive it results in effective spreading and a nice floating film of the polymer while a negative value of S results in balling of the polymer solution over the liquid substrate without spreading[40], [41]. The spreading phenomenon can also be expressed in terms of the following equations:

$$S = Y_1 - Y_2 - Y_{12} \quad \text{spreading coefficient} \quad (1.1)$$

$$S = Y_1 - Y_2 - Y_{12} < 0 \quad \text{No spreading} \quad (1.2)$$

$$S = Y_1 - Y_2 - Y_{12} > 0 \quad \text{Spreading of Polymer Film} \quad (1.3)$$

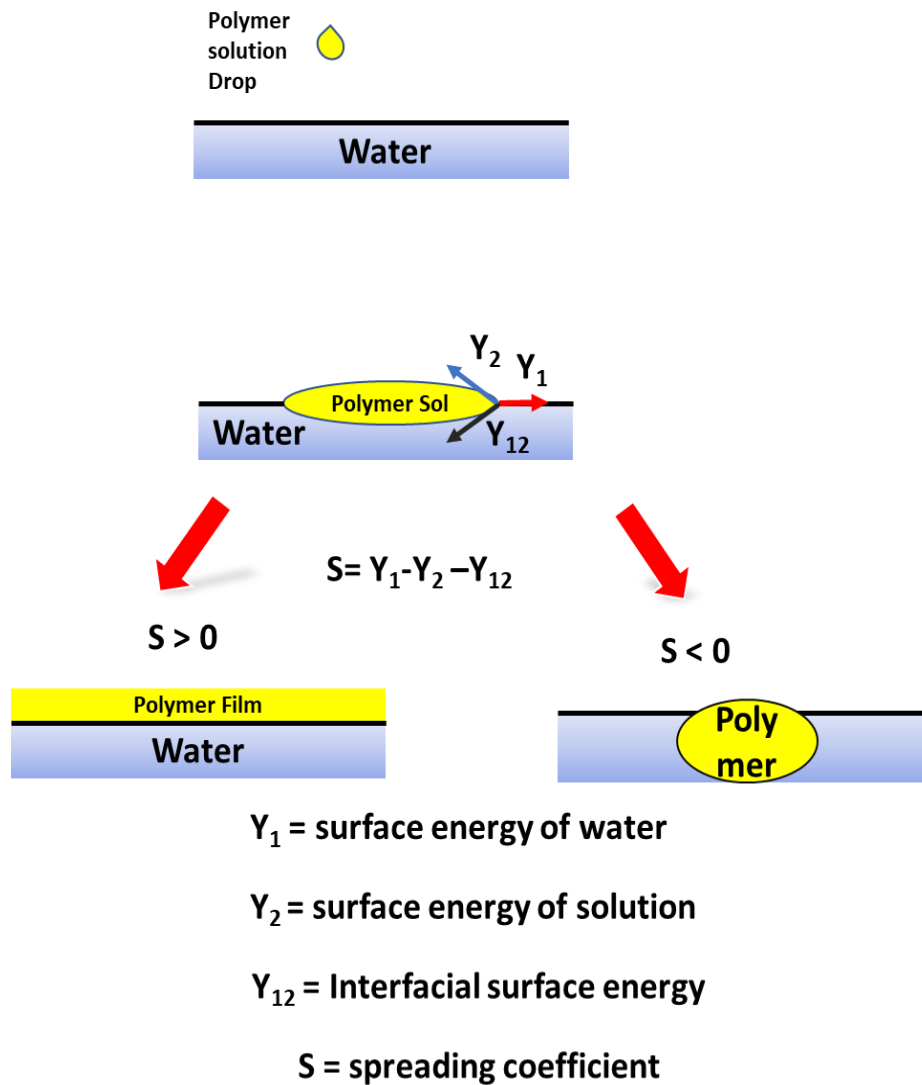


Figure 1.4 Steps in Floating film transfer Method

1.2.4 Brief Review of OFETs using FTM methods:

After being first reported by Kaneto and coworkers, the FTM method has been widely explored in the field of organic electronics. Here some significant works using FTM transferred film in the fabrication of OFETs have been briefly summarized. Morita et al in 2009[42] demonstrated a comparison between FTM transferred OFET and spin coated one. They used P3HT as an

organic semiconductor and a mixture of ethylene glycol and glycerol as a liquid substrate. The silicon dioxide based OFET with FTM transferred P3HT showed enhancement in mobility by an order of one, an increase in on/off ratio by more than an order of 2, and a reduction of the threshold voltage. Kumar et al in 2017[43] investigated FTM transferred PQT-12 based OFET (SiO₂ based high operating voltage OFETs) for ammonia gas sensing. Furthermore, they also compared the spin coated PQT-12 based OFET. The FTM transferred device recorded higher mobility, reduced threshold voltage, and increased on/off ratio. Like previous reports, they used a mixture of ethylene glycol and glycerol as a liquid substrate. The FTM transferred film shows a response of 56 % when compared with 24% of spin coated film on being exposed to 80 ppm of NH₃. The FTM processed film has a superior detection limit of 404 ppb while spin coated film has 814 ppb as the detection limit. Sahu et al. in 2017[44] investigated FTM transferred PBTTT-C14 based high voltage OFET for ammonia sensing. The dielectric material used in this experiment was CYTOP coated silicon dioxide. The processing of the FTM film included the use of ethylene glycol and glycerol as liquid substrates. The PBTTTC-14 FTM transferred OFET was operated at a very high voltage of V_{DS}=-60 V. The device showed a response of 89.84 % on exposure to 100 ppm of ammonia vapor while the lowest detection limit was 0.33 ppm and response and recovery time of ~26 s and 44 s were recorded. Kumar et al in 2018[45] studied the electrical and optical properties of FTM transferred PQT-12 for silicon dioxide based OFET. Like previous reports, the processing material in the liquid substrate was a mixture of ethylene glycol and glycerol. The device, which was operable at a high voltage of ~ -40 V, showed mobility of $\sim 7.8 \times 10^{-2}$ cm²/Vs, a threshold voltage of -8.3, and maximum responsivity of ~ 11.3 A/W at 5 μW/cm². Kumar et al in 2018 [46] studied CdSe

quantum dots and PQT-12 based nanocomposite for gas sensing performance. The OFET was fabricated using silicon dioxide dielectric with FTM transferred film of the nanocomposite. The liquid substrate for film transfer was a mixture of ethylene glycol and glycerol. The PQT-12 CdSe nanocomposite based OFET showed mobility of $4.2 \times 10^{-3} \text{ cm}^2/\text{Vs}$, the threshold voltage of -14.4 V , and an on/off ratio of $\sim 10^3$. The nanocomposite based OFET showed selective response of $\sim 51 \%$ to 100 ppm ammonia. Sung et al in 2020[47] demonstrated high performance OFET using the FTM method. They used water as the liquid substrate for film transfer. However, the device was working at a very high voltage and had poor subthreshold swing.

1.2.5 Review of Some OFET-based NO₂ Sensors.

Being one of the most hazardous pollutants NO₂ is the main cause of acid rain, photochemical smog, and eutrophication. Common sources of NO₂ include automobile exhaust, chemical, and food processing industries. Nitrogen dioxide is extremely hazardous to human health and the environment[48], [49]. The Environmental Protection Agency (EPA) has set a yearly national ambient air quality limit of 53 parts per billion (ppb) for NO₂. This standard denotes the official maximum allowable amount of this pollutant in the air that is considered safe to inhale. Additionally, nitrogen oxide (NO_x) detection could serve as a beneficial diagnostic tool. Nitric oxide, for instance, can be detected in exhaled breath to help diagnose lung tissue infections. Nitric oxide levels in the exhaled breath significantly increase three to five times before an asthma episode[50], [51]. People with asthma would have the chance to take preventative treatment if they could use a portable gadget to check their nitric oxide levels at home. As a result, the need for portable, efficient, and cost-effective point-of-care devices capable of

detecting NO₂ at extremely low levels is obvious in helping with patient diagnosis. Organic thin-film transistors (OTFTs)-based sensors for gases have garnered significant interest due to inherent benefits such as cheap cost, lightweight, flexibility, stretchability, and possible biocompatibility. Furthermore, because OTFT has several electrical parameters and its performance can be easily modified using the field effect, it works well as both a signal transducer and an amplifier[52]. Li et al[49] in 2015 reported enhanced NO₂ sensing performance by inserting a silk fibroin layer as dielectric over PMMA. The result demonstrated that employing silk fibroin as bilayer dielectric over PMMA improved sensing performance. The enhanced sensing due to silk fibroin was attributed to large density of hydroxyl ions as surface trap which helped in more interaction with gas molecule. However, the device has very large voltage of operation and sensitive only in the range of 10 ppm onward. In 2016 Yang et al [53] reported P3HT, graphene oxide (GO) and zinc oxide (ZnO) nanocomposite based OFET for NO₂ sensor. They used spin coating for depositing hybrid nanocomposite. The P3HT/GO/ZnO nanocomposite based OFET showed a response of 210 % at 5 ppm of NO₂.

Han et al in 2018 reported [48] NO₂ sensor by utilizing poly(9-vinylcarbazole) (PVK) as a hole transporting or electron blocking blend for enhancing sensing performance. The P3HT/PVK combination provides increased responsiveness and sensitivity, as well as superior selectivity and performance. In this system, PVK serves a dual purpose by enhancing the adsorption interface of P3HT and aiding the extraction of additional holes generated by traps. The NO₂ responsivity of OFETs with a 1:1 P3HT/PVK mixture exceeds 20,000% for 30 ppm (at -40 V).

Xie et al in 2019 reported [52] reported an Al₂O₃/PMMA bilayer based NO₂ sensor utilizing heterojunction of p-6P and CuPc organic semiconductors. The device showed almost ~1000 % response at - 2 V for 20 ppm of NO₂. They observed that different molar concentrations of

Al_2O_3 precursor resulted in different responses. Zhu et al [51] in 2021 investigated the different combinations of bilayer polymer dielectric for NO_2 sensing performance utilizing p-6P and CuPc active layer. A combination of PMMA with polystyrene (PS), polyvinyl pyrrolidone (PVP), and PMMA was spin coated. When exposed to a 30 ppm concentration of NO_2 gas, the sensors' responsivity increases significantly in the case of PMMA/PS to 7633% in comparison to PMMA/PMMA bilayer (5624%) at $V_{\text{DS}} = -50$ V. Additionally, the sensitivity increases noticeably, rising from 198% per ppm to 265% per ppm. Yu et al [54] in 2019 reported DPP-DTT based NO_x sensor using the breath figure molding technique to enhance NO_2 sensing performance. Breath figure molding (BFM) is commonly used to obtain precise control over the level of nano porosity in the polymer film. The BFM technique is not suitable for large area processing. Additionally, it requires strict humidity control thereby requiring a costly humidity control setup. The fabricated device using BFM shows around 40000 % change on exposure to 10 ppm of NO_2 .

1.2.6 Review of Some NIR Phototransistors.

Due to the wide range of applications ranging from thermal imaging to night vision and health safety monitoring, near-infrared (NIR) photodetectors have gained attention in recent years [55]. Out of various configurations of photodetectors (photoconductor, photodiode, and phototransistors), phototransistors are most preferred because of the advantage of amplification. Just by adjusting the gate voltage, phototransistors can provide high gain with little noise. As the NIR light has the tendency to penetrate human tissue, the NIR phototransistors are commonly used in health monitoring systems like cardiovascular

monitoring systems or pulse oximetry. Furthermore, owing to the availability of a third terminal it is easier to integrate phototransistors with data-collecting circuits[55]–[57]. Some key parameters of phototransistors have been discussed below:

Photoresponsivity: The photoresponsivity (R) parameter is calculated by dividing the photocurrent detected in a photodetector by the incident optical power. Photoresponsivity measures the efficiency with which photons are converted into electrical charge. It may be expressed mathematically as follows[55]:

$$R = \frac{I_{photo} - I_{dark}}{AP_{in}} \quad (1.4)$$

External Quantum efficiency (EQE): The EQE quantifies the efficiency of converting light to electricity, at a particular wavelength of light. It is determined by the ratio of the number of photo-generated charge carriers extracted to the number of incident photons. The mathematical expression for the calculation of EQE is given by[55]:

$$EQE = \frac{Rhc}{\lambda} \quad (1.5)$$

Photosensitivity (P): is the ratio of the channel current in phototransistors when exposed to light compared to when not exposed to light, which indicates the level of photo-switching.

This is how it is defined[55]:

$$P = \frac{I_{photo} - I_{dark}}{I_{dark}} \quad (1.6)$$

Specific Detectivity: Detectivity is another parameter that is used to determine the performance parameters. It is denoted by D^* and is related with responsivity (R), dark current (I_{dark}) and illuminated area (A).

$$D^* = \frac{R\sqrt{A}}{\sqrt{2qI_{dark}}} \quad (1.7)$$

Where I_{photo} , I_{dark} , A, q, h, c, and λ represent photon current, dark current, illuminated device area, the charge on an electron, plank constant, velocity of light, and peak wavelength of light

Zhu et al [58] in 2016 fabricated NIR OPTs using nanowires of polymer (PBIBDF-TT). Under NIR light of 47.1mW/ the p-type device of nanowire-based PBIBDF-TT NW-OPTs shows remarkable photosensitivity of $\sim 1.3 \times 10^4$ and responsivity of 440 mA/W. The increased photosensitivity is attributed to the trap charges at the semiconductor dielectric interface and the semiconductor air interface due to the increased surface to volume ratio owing to nanowires. Lei et al in 2017[59] reported highly sensitive organic phototransistors (OPTs) that function in the near-infrared (NIR) region using nanowire networks. These OPTs make use of a photoactive channel made of a donor-acceptor (D-A) polymer with a small bandgap. When exposed to NIR light at 850 nm with an intensity of around 0.1 mW/cm², NIR-OPTs based on the D-A polymer nanowire network exhibit a remarkable responsivity of about 246 A/W. Several reasons contribute to the outstanding performance of phototransistors based on nanowire networks. These include a remarkable ability for hole transport, reduced density of structural defects in polymer nanowires, and improved contact between the channel layer and

electrode interfaces. Wang et al in 2018[56] reported NIR OPTs using n-type polymer (PBIBDF-BT) utilizing trap charges available at AlO_x dielectric surface. They passivated trap charges using different durations of treatment for self-assembled monolayers of octadecyl phosphonic acid. The performance enhancement in photosensitivity ($\sim 5 \times 10^3$) was attributed to trap charges present on AlO_x surface. The higher the trap charges higher was the value of photosensitivity. The device worked at a lower voltage of ~ 5 V but the responsivity value of only 20 mW/A was obtained. Wang et al in 2020 [60] reported DPP-DTT nanowire based NIR OPT with an operating volage of ~ -3 V. This report used 6-azide-hexyl phosphonic acid SAM monolayer treatment over the AlO_x surface to paasivate trap charges. The devices showed a photosensitivity of 2.25×10^4 , and a responsivity of 0.10 A/W at 808 nm at the intensity of 48.25 mW/cm². Yang et al[61] in 2020 reported PbS quantum dots doped P3HT based NIR OPTs using PMMA dielectric layer. The devices recorded a responsivity of 0.0094 A/W at the wavelength of 980 nm and at an intensity of 200 mW/A ($V_{DS} = -10$ V $V_{GS} = -40$ V). Kim et al in 2022 reported NIR OPTs using a blended gate sensing layer with conjugated and insulating blend[62].

1.3 Motivation

The use of OFETs in IoT and portable hand-held sensors has gained much attention in recent years. Portability and low power constraints require low voltage operable OFETs. Many high k inorganic dielectrics have been employed as gate dielectrics to lower the operating voltage. LiO_x , an inorganic gate dielectric, that has been employed to fabricate indium oxide based TFTs[6], [7], [16]–[25], [8]–[15] has not been explored as the gate dielectric in organic

semiconductors. Due to the availability of a high density of surface charge traps and comparatively rough surface, integration of inorganic dielectrics with organic semiconductors is a challenging task [63]. Recently Lithium has been extensively used in electric batteries and in due course of time if some methods or technology comes out that can recycle the Lithium-ion wastes to a favorable precursor of Lithium, it can be used to prepare LiOx. This has been one of the motivations to explore the usability of LiOx as a dielectric in OFET. Furthermore, the majority of reported inorganic dielectrics for Organic semiconductors have been processed through toxic organic solvents making the whole process harmful and environmentally damaging. Water based processing of inorganic dielectrics is an exciting domain that can make the processing eco-friendly. The commonly used solution processing technologies for organic semiconductor like spin coating, spray coating, and printing require costly and sophisticated instruments and results in material wastage limiting their use in large area low-cost electronics. Recently Floating film transfer method has gained popularity owing to its advantages like large area processing suitability, no requirement of complex instruments, minimal wastage of organic semiconductor material, and availability of highly ordered film. Commonly used liquid substrates in the FTM method are ethylene glycol, glycerol, and water. However, the use of ethylene glycol and glycerol makes the process environmentally damaging. Water substrate has the advantage of being eco-friendly. Water-based FTM processing is least explored for application in OFETs. Despite all the advantages of FTM most of the reports of FTM-based OFETs have explored the sensing application and very little attention has been done to develop high performance low voltage OFETs. Furthermore, the integration of water-based OSC FTM processing and water induced dielectric processing can result in near eco-friendly processing of OFETs. Since the most common applications of

OFETs include gas sensing and light sensing, this area with eco-friendly processing needs further exploration. NO₂ is one of the most hazardous gas and can cause cardiovascular and respiratory impairment while it is also being used as a biomarker. So, the development of an eco-friendly processed OFET based NO₂ sensor for ppb level detection limit is much needed. In addition, DPP-DTT being a polymer sensitive to the NIR region can be utilized to fabricate a NIR phototransistor. Furthermore, since NIR photodetectors find application in health monitoring like pulse oximetry, the development of low voltage NIR phototransistors is the need of the hour considering the portability and low power requirement in health monitoring systems. Hence the integration of water transferred FTM film and water processed synthesis of the dielectric layer has been done followed by the investigation of W-FTM transferred DPP-DTT for some low power NO₂ sensing and low power high performance NIR OPTs.

1.4 Problem Statement

Enormous progress has happened in the field of solution-processed OFETs in terms of processing. Based on the extensive literature review as summarized in the previous section following research gaps and challenges have been enlisted in this section.

1. Lithium oxide has moderate dielectrics constant but it has not been explored for dielectrics in Organic FETs. Reports of the utilization of water-processed inorganic dielectrics in OFETs are rare. This motivated us to investigate water-induced LiOx as the gate dielectric.
2. Water-induced processing of dielectric is superior and eco-friendly. There have been many reports of water-processed inorganic dielectrics for inorganic semiconductors. However, its integration with Organic semiconductors has rarely been studied.

3. There is a need for the development of Low power operable OFETs with good performance parameters along with the added advantage of eco-friendly and low-cost processing techniques. The majority of the solution-processed techniques for OSC are unsuitable for large area electronics and the previous reports using FTM for OFET fabrication have either very high voltage of operation or poor performance metrics (SS, ON/OFF ratio).
4. To explore low-cost, cost-effective Water based FTM technology for OSC and its efficient integration with Water Induced Gate Dielectric for large area electronics and low voltage operable systems.
5. Despite its eco-friendly advantage and large area suitability, W-FTM has rarely been used for gas sensing and photodetection. To explore the application of W-FTM transferred DPP-DTT film for high performance ppb level NO₂ sensor and near-infrared organic phototransistor by following nearly eco-friendly processing.

There are very few reports exploring the electrical stability of the devices along with low voltage operation. This is because the use of high k dielectric generally degrades electrical stability due to surface charge traps.

1.5 The objective of the Thesis

1. To explore water processed LiO_x dielectric for the fabrication of high performance OFETs.
2. To integrate water processed dielectric and large area suitable FTM method utilizing water transferred OSC film for fabrication of OFETs. Thereby approaching towards completely eco-friendly processing of OFETs.

3. To further improve the performance (ON/OFF ratio, SS, mobility) of LiO_x based OFETs using bilayer dielectrics.
4. To design OFET with high performance parameters with ultra-low voltage operation.
5. To explore the application of W-FTM transferred and DPP-DTT film for high-performance ppb level NO_2 sensor by following nearly eco-friendly processing.
6. To investigate and design high performance ultra-low voltage (Eco-friendly processed) near infra-red organic phototransistors (NIR OPTs) with high performance parameters (High Responsivity, EQE).

1.6 Some basics of OFETs and parameters

1.6.1 Charge Transport in Organic Semiconductors:

The primary feature that provides organic molecules the ability to conduct electrical charge is molecular conjugation, which is the existence of alternate (σ) single and double (π) bonds between covalently bonded carbon atoms. One valence electron (out of 4 electrons) from each carbon atom participating in the conjugated system is delocalized as a result of this conjugation, enabling effective electronic charge transfer along the conjugated molecule. Organic semiconductors as discussed before can be classified as small molecules and polymers. Charge transport mechanisms in organic semiconductors can be broadly classified into two types band to band transport and hopping model[3], [4].

1.6.1.1 Band Transport:

The band-to-band transport, which features the delocalized wave function over the whole system thereby leaving the electron position nothing more than a wavefunction probability, results in coherent transport thereby making it an extremely quick process. One important feature of band-like transport is a decrease in mobility with increasing temperature (T) which is generally observed in single-crystal films. The variation of mobility (μ) with temperature (T) follows power law ($\mu \propto T^{-n}$) where $0.5 < n < 3$ n is a fitting parameter, μ is mobility and T is temperature). Such band-to-band transport is generally observed in vapor-processed single-crystal films and solution-processed TIPS-Pentacene films[3], [4].

1.6.1.2 Hopping Transport:

The hopping form of charge transport in organic semiconductors is generally characterized in which electron functions as a localized carrier whose motion is restricted to a specific molecule or short segment of chain and observed as small hops thereby resulting in the incoherent form of transport. The cases when organic semiconductors have a large density of traps like amorphous or polycrystalline thin films the hopping transport is the dominant mechanism which is characterized by tunneling between the localized states. In the hopping form of transport, mobility is a direct function of temperature.

In practice, the charge transport in organic semiconductors can be considered as a combination of both models as described above. Many efforts have been made to integrate both models into

a single equation showing a seamless transition between both states. At lower temperature band-to-band transport predominates while with rising temperatures the hopping model comes into the picture. In this case, the room temperature is considered a critical transition temperature. Below the room temperature band-like model is dominant while at a temperature higher than the room temperature hopping model comes into effect[3], [4].

1.6.2 Basic Structures of OFETs and Region of Operations

Since OFET includes many layers arranged one over another layer namely: OSC, the Gate dielectric, and Contacts, variation in arrangement layer based on their sequential deposition can give rise to different structures. Broadly Speaking the OFET structures can be classified as Bottom Gate Bottom Contact (BGBC), Bottom Gate top Contact (BGTC), Top Gate Bottom Contact (TGBC), and Top Gate top Contact (TGTC). Based on the planar location of the Organic semiconductor channel, Source, and drain, these four structures can be further classified as planar (BGBC and TGTC) or staggered (TGBC and BGTC). The bottom gate structure exposes the semiconducting layer to the ambient and thus has inherent stability issues however these structures are more suitable for solution-processed routes [3]. Figure 1.5 shows all the configurations of OFETs.

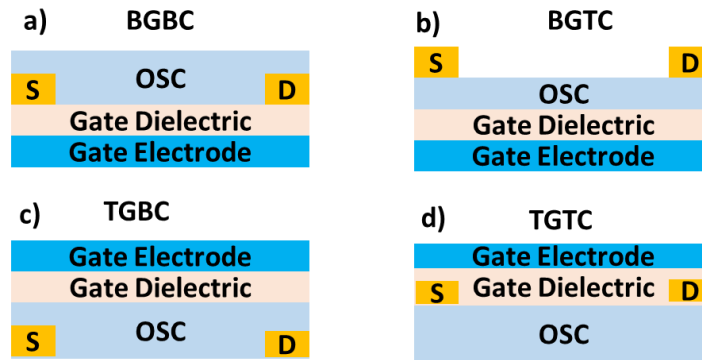


Figure 1.5 Structures of OFETs.

Furthermore, the OFETs can have three regions of operation namely linear region, pinch-off, and, saturation as shown in Figure 1.6. Application of negative gate voltage (V_{GS}) results in the accumulation of holes at the OSC/dielectric interface in the case of p-type OFETs. Whereas the application of negative V_{DS} (more than the threshold voltage) helps in the transportation of holes. When $V_{DS} = 0$ and $V_{GS} < 0$, the accumulated holes are distributed uniformly but $I_{DS} = 0$ since there is no driving force. When a very small V_{DS} ($V_{DS} \ll |V_{GS} - V_{TH}|$) is applied it results in linear variation in channel charge density from the source terminal to drain which further results in a linear increase in drain current with increasing V_{DS} [3], [64]. This region of operation is called the linear region. When V_{DS} is further increased such that $V_{DS} = |V_{GS} - V_{TH}|$ then a pinch-off region appears around the drain terminal resulting in the formation of a depletion region. When V_{DS} is increased beyond the pinch-off voltage the drain current doesn't increase significantly. Therefore, this is called saturation region[3], [64].

1.6.3 Working Principle of OFETs

In this section basic working of OFETs is described. The working of OFETs can be better understood using different cases. For a better understanding of working, Figure 1.7 have been used considering both the cases for n-type and p-type.

Case 1 When $V_G = 0$ and $V_{DS} = 0$ there is no induced charge in the channel of undoped organic semiconductor so there will be no conduction. This is because OSCs are generally undoped intrinsically. So conduction requires the induction of charges by applying proper gate voltage[3], [65], [66].

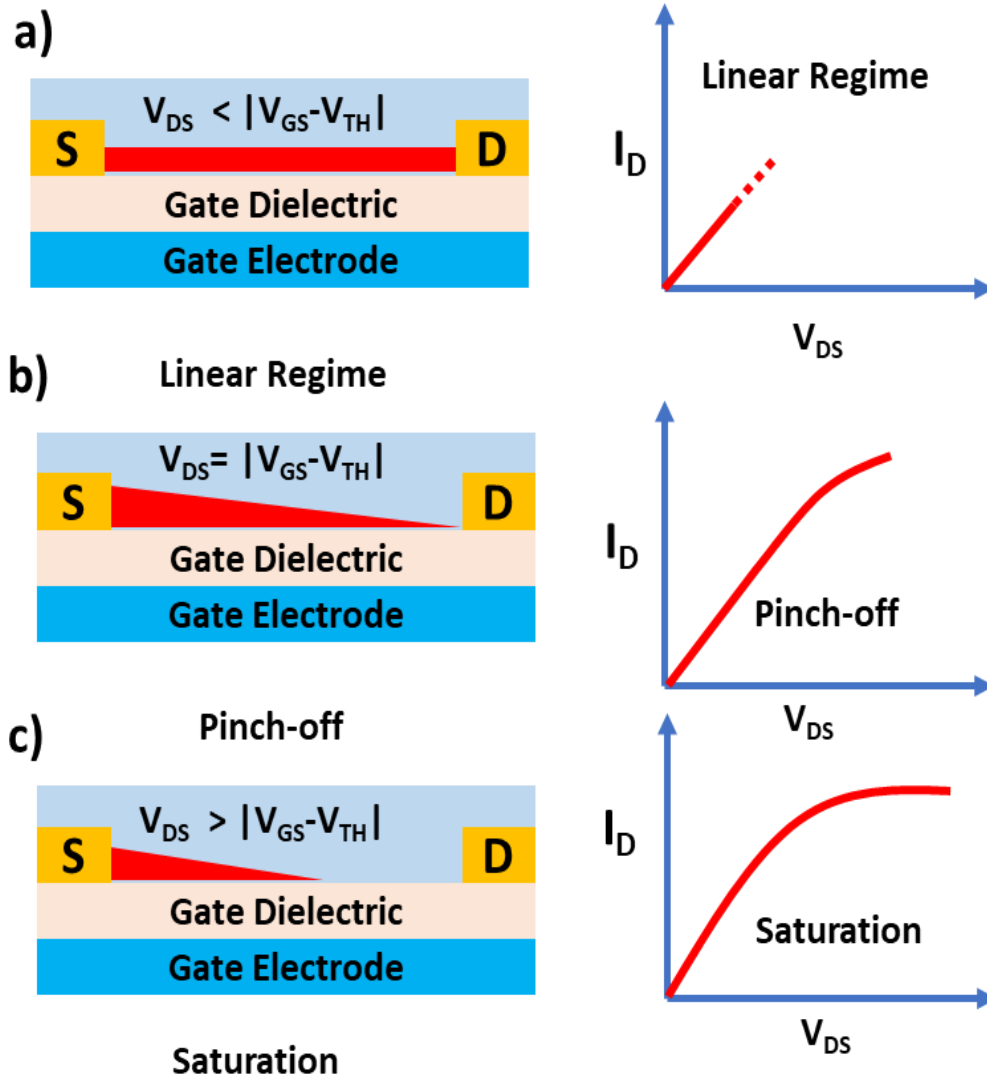


Figure 1.6 (a) Region of operation of OFETs and current-voltage characteristics (a) Linear Region (b) Beginning of saturation at pinch-off voltage; (c) saturation regime condition.

Case 2 P-type material:

When $V_G < 0$ and $V_D = 0$ application of negative gate voltage results in upward shifting of HOMO and LUMO levels so that the HOMO level becomes resonant with the Fermi level of

source drain contact and subsequent induction of positive charges at the OSC/dielectric interface. This is also called hole accumulation or the formation of a p-type conducting channel. The hole injection and extraction can happen by applying a suitable voltage at drain source electrode ($V_{DS} < 0$). However, for efficient hole injection, the Fermi level of the metal electrode at the source drain should be close to the HOMO level of OSC. Such organic semiconductors are called p-type semiconductors. [3], [65], [66]

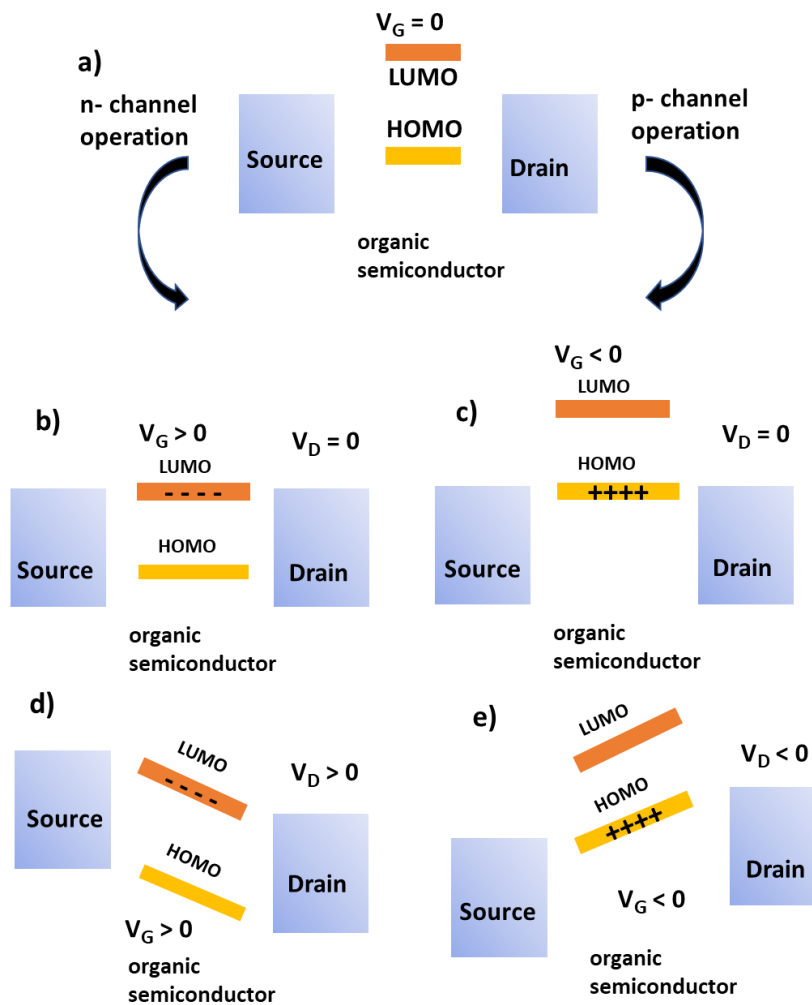


Figure 1.7 Basic working of OFETs

Case 3 n-type material: When $V_G > 0$ and $V_D = 0$ application of positive gate bias results in the downward shifting of HOMO and LUMO levels so that the LUMO level becomes resonant with the fermi level of source-drain contact followed by induction of negative charges at the OSC/dielectric interface. This is termed as electron accumulation. The electron injection and extraction can happen by applying a suitable voltage at the drain-source electrode. However, for efficient electron injection, the Fermi level of metal contact at the source-drain should be close to the LUMO level of the OSC. Such OSCs are generally known as n-type materials.[3], [65], [66].

1.6.4 Performance Parameters of OFETs

The mobility (μ), subthreshold swing (SS), trap density (N_{it}), and on/off ratio are some of the key performance parameters of the OFETs. All these parameters are extracted using either the semilog drain and V_{GS} plot or the square root of $I_D - V_{GS}$ plot as depicted in Fig 1.8. The extraction of these parameters is described below[3], [67]:

Field-effect mobility (μ): In order to obtain the saturation mobility, the square root of the drain (I_D as given by equation 1.8) current is plotted with respect to the gate voltage. Then the square root of the drain current and gate voltage curve is linearly fitted. The maximum slope of the linear fit is used to calculate the mobility using equation 1.9[3], [67]. The variables q , W , L , and kT stand for the charge on an electron, channel width, channel length, and thermal energy, respectively. The variables C_i , I_D , and V_{GS} stand for the capacitance per unit area of the gate dielectric, drain current, and gate-source voltage.

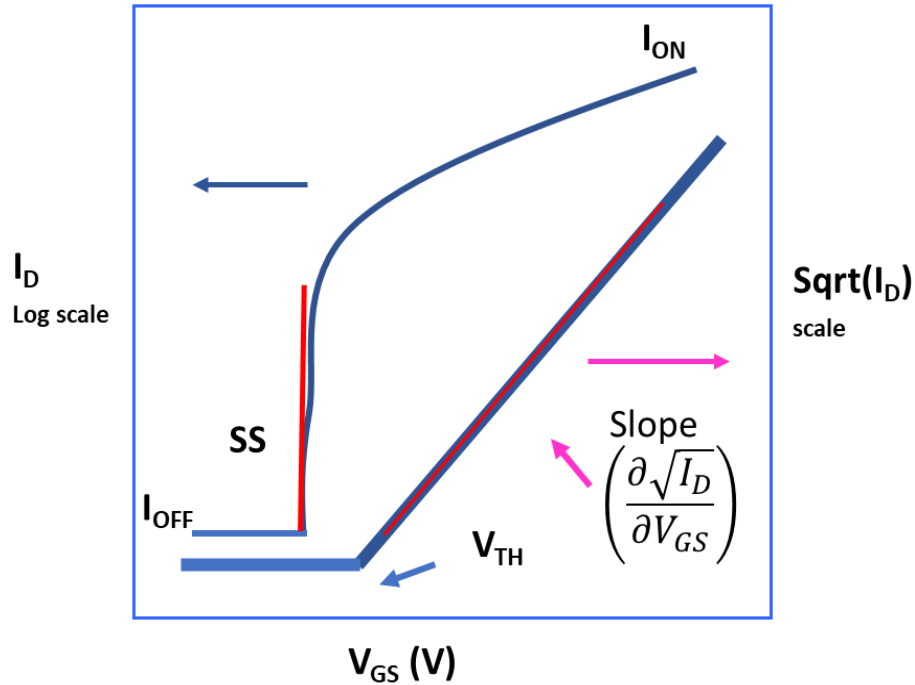


Figure 1.8 Transfer Characteristics of a representative OFET.

$$I_D = \frac{\mu C_i W}{2L} (V_{GS} - V_{TH})^2 \quad (1.8)$$

$$\mu_{sat} = \frac{L}{C_i W V_{DS}} \left(\frac{\partial \sqrt{I_D}}{\partial V_{GS}} \right)^2 \quad (1.9)$$

$$C_i = \frac{k \epsilon_0 A}{d} \quad (1.10)$$

Subthreshold Swing (SS): When the gate voltage is less than the threshold voltage the operating region is called the subthreshold region which is characterized by the exponential rise in drain current. In this region, the drain current is governed by the charge carriers having sufficient thermal energy to break through the gate voltage-controlled energy barrier. The subthreshold swing (SS) is given by [3], [67] :

$$SS = \left(\frac{d \log(I_D)}{dV_{GS}} \right)^{-1} \quad (1.11)$$

Trap Density (N_{it}):

Another important parameter of OFETs is trap density. Subthreshold swing can be used to estimate the trap charge density (N_{it}) at the dielectric semiconductor interface using equation 1.12. The smaller the trap density smaller will subthreshold swing resulting in a steep rise in the slope in the subthreshold region[3], [67].

$$N_{it} = \left(\frac{\log e \cdot SS}{\frac{kT}{q}} - 1 \right) \frac{C_i}{q} \quad (1.12)$$

ON/OFF Ratio:

Another significant parameter for OFET performance is on /off ratio also called the switching ratio. In order to calculate the on/off ratio the logarithmic plot of I_D versus V_G is used with the ratio of maximum to minimum current. The switching ratio reflects the ability of OFETs to effectively turn off and is useful in many applications which use OFET as a switch[3], [67].

1.7 Materials and Methods

Although details of the material used and fabrication steps have been already covered in the published papers, for better pictorial representation and flow this section briefly presents the experimental details and materials used in all experiments.

1.7.1 Steps of OFET fabrication used in this thesis:

Figure 1.9 represents the basic steps used in the fabrication of solution processed OFETs that have been used in this thesis in the following chapters. P-type Silicon substrate has been utilized as the gate electrode and substrate followed by ultrasonically cleaning using isopropyl alcohol and acetone. Plasma cleaning of the substrate has been done to improve adherence to the dielectric precursor solution. The spin coated dielectric solution has been annealed followed by FTM transfer of the OSC layer. Finally Gold source drain electrode has been deposited over the FTM transferred organic semiconductor film using Ossila metal masks. The electrical characterization has been carried out using Agilent B1500A semiconductor parameter analyzer.

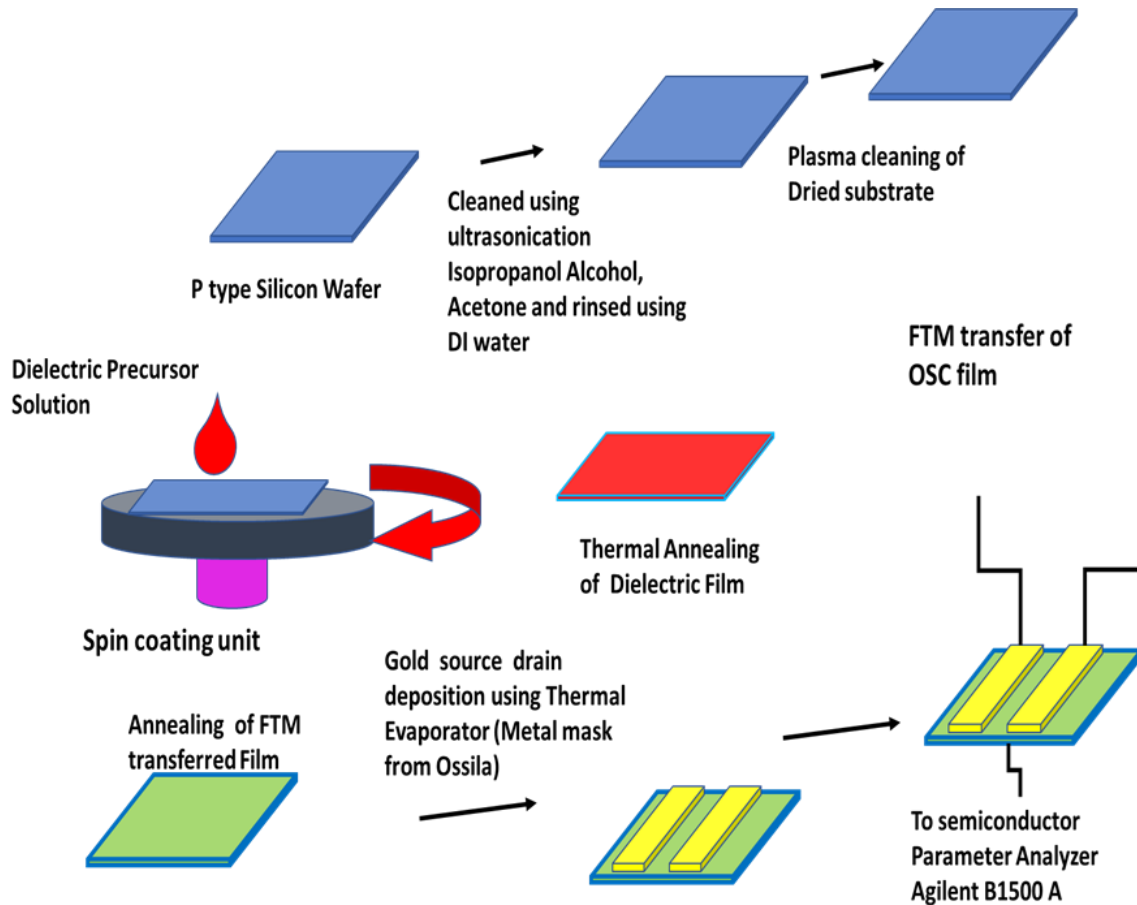


Figure 1.9 Steps in Fabrication Process.

1.8 Scope of the Thesis

The significance and basic working of Organic field effect transistors have been covered in this thesis along with the charge transport mechanism, performance parameters, device structure, and basic working steps. A summary of significant and recent research on high k inorganic dielectrics in OFETs, water processed dielectrics, OFET-based NO_2 sensors, and NIR phototransistors along with performance parameters has been presented. Furthermore, a brief detail of the FTM method and its basics has been also included followed by the details of the fabrication steps used in this thesis. This thesis consists of 6 chapters including the current one. A brief outline of the chapters has been covered below:

Chapter 2 includes the fabrication and characterization of water induced LiO_x based OFETs. Basic morphologies of dielectric and organic semiconductor film, Leakage and capacitance behavior of water induced LiO_x dielectric have been presented. A detailed electrical characterization along with OFET parameter extraction has been presented.

Chapter 3 is devoted to the fabrication and characterization of bilayer dielectric based ultra-low voltage operable OFETs. This chapter briefly covers the introduction, experimental details, characterization of bilayer dielectric film (leakage behavior, areal capacitance, and bandgap calculation), transfer characteristics of the $\text{LiO}_x/\text{AlO}_x$ based OFET along with current bias stability.

Chapter 4 investigates W-FTM transferred ultrathin DPP-DTT film for NO_2 sensing using water processed AlO_x based low voltage operable OFET. Starting with a brief introduction the chapter discusses sensing response, a multiparametric variation on exposure to different

concentrations of nitrogen dioxide followed by the analysis of the effect of humidity on sensing response, selectivity, and transient analysis.

Chapter 5 covers W-FTM transferred DPP-DTT based NIR OPT using biocompatible water-processed PVA dielectrics. Starting with a brief introduction this chapter deals with the basic characterization of the PVA dielectric layer followed by UV -vis -NIR analysis of W-FTM transferred DPP-DTT and electrical and optical characterization of NIR OPT. The responsivity, external quantum efficiency, and, detectivity of the NIR OPTs have been calculated and compared with recently reported OPTs.

Chapter 6 Finally this chapter presents an insightful summary of all the experimental chapters, the contribution of this thesis with possible future scope of the current work.